Acta Crystallographica Section F
Structural Biology and Crystallization Communications
ISSN 1744-3091

Crystallization and preliminary crystallographic analysis of nosiheptide-resistance methyltransferase from *Streptomyces actuosus* in complex with SAM

Huirong Yang,[a,b,c]‡ Ping Wang,[b,c]‡ Zhenghong Dong,[b,c,d]‡ Xueyuan Li,[e] Rui Gong,[b,c] Ying Yang,[b,c] Ze Li,[b,c] Youwei Xu[b,c] and Yanhui Xu[a,b,c]*

[a]Department of Pathology, Cancer Hospital, Fudan University, Shanghai 200032, People's Republic of China, [b]Institutes of Biomedical Sciences, Fudan University, 130 Dong-An Road, Shanghai 200032, People's Republic of China, [c]School of Life Sciences, Fudan University, 220 Han-Dan Road, Shanghai 200433, People's Republic of China, [d]Department of Chemistry, Fudan University, 220 Han-Dan Road, Shanghai 200433, People's Republic of China, and [e]Neurosurgery Department, Liaocheng People's Hospital, Shandong Province 252000, People's Republic of China

‡ These authors contributed equally to this research.

Correspondence e-mail: xuyh@fudan.edu.cn

Received 21 January 2010
Accepted 25 March 2010

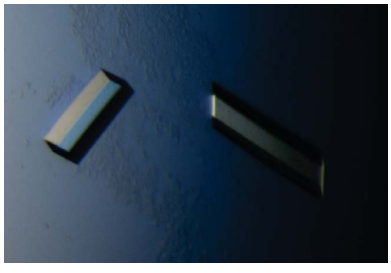

Nosiheptide-resistance methyltransferase (NSR) methylates 23S rRNA at the nucleotide adenosine 1067 in *Escherichia coli* and thus contributes to resistance against nosiheptide, a sulfur-containing peptide antibiotic. Here, the expression, purification and crystallization of NSR from *Streptomyces actuosus* are reported. Diffracting crystals were grown by the hanging-drop vapour-diffusion method in reservoir solution consisting of 0.35 *M* ammonium chloride, 24%(*w*/*v*) PEG 3350, 0.1 *M* MES pH 5.7 at 293 K. Native data have been collected from the apo enzyme and a SAM complex, as well as apo SeMet SAD data. The diffraction patterns of the apo form of NSR, of NSR complexed with SAM and of SeMet-labelled NSR crystals extended to 1.90, 1.95 and 2.25 Å resolution, respectively, using synchrotron radiation. All crystals belonged to space group $P2_1$, with approximate unit-cell parameters a = 64.6, b = 69.6, c = 64.9 Å, β = 117.8°.

1. Introduction

Bacterial resistance to antimicrobial agents is an increasingly important problem. Resistance to their own antibiotics has been observed in some drug-producing strains such as *Streptomyces actuosus*, *S. antibioticus* and *S. glaucogriseus*, which produce nosiheptide. Nosiheptide is a sulfur-containing peptide antibiotic with a molecular weight of 1222 Da that belongs to a family of thiazole antibiotics (Prangé *et al.*, 1977; Endo & Yonehara, 1978). It has been used in veterinary medicine as a treatment against Gram-positive bacteria and has poor solubility (Cromwell *et al.*, 1984). Other sulfur-containing peptide antibiotics include thiostrepton, siomycin, sporangiomycin *etc*. They are closely related in structure to nosiheptide and possess identical modes of action (Thompson & Cundliffe, 1980). Nosiheptide irreversibly binds to 50S subunits of ribosome and inhibits the hydrolysis of guanosine 5′-triphosphate (GTP) by elongation factor G (EF-G), thus inhibiting elongation (Wimberly *et al.*, 1999; Harms *et al.*, 2008). Since nosiheptide binds 23S ribosomal RNA (rRNA; Harms *et al.*, 2008), self-protection is required for normal translation in its producer strain. *S. actuosus* immunizes itself with the 23S rRNA methyltransferase nosiheptide-resistance methyltransferase (NSR), which contributes to resistance against nosiheptide by methylation at 2′-OH of adenosine 1067 (Li *et al.*, 1990). It has been reported that nucleotides 1051–1108 of 23S rRNA in *Escherichia coli* are the natural substrate of NSR (Bechthold & Floss, 1994). The sequence is composed of a terminal stem, 1067 stem-loop, 1082 hairpin and 1095 stem-loop (Gutell *et al.*, 1994; Lentzen *et al.*, 2003; Robinow & Kellenberger, 1994).

From amino-acid sequence analysis using Pfam (Finn *et al.*, 2008), NSR is predicted to be composed of an N-terminal RNA-binding domain (NTD; residues 1–107) and a C-terminal catalytic domain (CTD; residues 108–274) which binds *S*-adenosyl L-methionine (SAM), a universal methyl donor for methylations mediated by methyltransferases (MTases; Roje, 2006). To date, five distinct classes of SAM-dependent MTases have been identified based on structural differences. NSR belongs to the class IV SPOUT-family MTases, which also contains the SpoU (TrmH including single domain or with the addition of ribosome large subunit L30 and L5 domains) and the TrmD [tRNA methyltransferase including single domain or with

the addition of a TRP (tryptophan repressor) domain] subfamilies (Mosbacher *et al.*, 2005).

RNA MTases have been identified as clinically significant resistance determinants to a number of antibiotics. For example, AviRb (avilamycin resistance factor b) from *S. viridochromogenes* mediates resistance to the oligosaccharide antibiotic avilamycin (Mosbacher *et al.*, 2005), Erm is responsible for macrolide–lincosamide–streptogramin resistance (Farrow *et al.*, 2000), 16S rRNA methyltransferase FmrO from *Microspora olivasterospora* is involved in fortimicin A resistance (Ohta & Hasegawa, 1993), RlmB from *E. coli* has been predicted to inhibit certain antibiotics (Michel *et al.*, 2002) and TSR (thiostrepton-resistance methyltransferase) from *S. azureus* has been reported to be resistant to thiostrepton (Dunstan *et al.*, 2009). The structures of several of these RNA methyltransferases have been reported. However, the structure of NSR and more importantly the molecular mechanism of NSR-mediated 23S rRNA methylation remain unknown.

Here, we report the expression, purification, crystallization and preliminary crystallographic studies of native NSR, of NSR in complex with SAM and of selenomethionine-derivative NSR.

2. Materials and methods

2.1. Protein expression and purification

The cDNA encoding full-length *nsr* (GenBank U75434.1) was amplified by PCR using genomic DNA from *S. actuosus* (a gift from Professor Alastair Murchie, Fudan University, People's Republic of China) as the template and then inserted into the pETduet vector (Novagen) (using the DH5α strain) using *Eco*RI and *Xho*I restriction sites. The construct was verified by sequencing and the plasmid was transformed into *E. coli* strain BL21 (DE3) competent cells. The transformants were grown at 310 K to an OD_{600} of 0.6 in Luria broth medium containing 100 mg l^{-1} ampicillin and were induced by adding 0.1 m*M* isopropyl β-D-1-thiogalactopyranoside. NSR was expressed as a fusion protein with a His tag at the N-terminus. After a further 12–16 h incubation at 289 K, the cells were pelleted and resuspended in lysis buffer containing 25 m*M* Tris pH 8.0, 150 m*M* NaCl and 5 m*M* imidazole supplemented with DNAse and protease inhibitors. The cells were lysed on ice using a French press and the solution was clarified by centrifugation at 12 000 rev min^{-1} for 25 min at 277 K. The supernatant was applied onto six Ni–NTA columns (1 ml resin per column; GE Healthcare) pre-equilibrated with lysis buffer. After washing with buffer containing 25 m*M* Tris pH 8.0, 150 m*M* NaCl and 20 m*M* imidazole, the fusion protein was digested on the column with TEV protease for 4 h at 277 K. The molecular weight of the digested protein was 29 547 Da including the additional Ser-Glu-Phe from the TEV cleavage site and *Eco*RI restriction site. The eluted protein was then loaded onto a Source 15Q anion-exchange column (GE Healthcare) and eluted with a linear gradient of 0–0.5 *M* NaCl at a flow rate of 10 ml min^{-1}. The peak fractions were collected and further purified by gel-filtration chromatography on a Superdex 200 column (GE Healthcare) with buffer containing 10 m*M* HEPES pH 7.5, 250 m*M* NaCl and 5 m*M* dithiothreitol (DTT). NSR-containing fractions were adjusted to 10 mg ml^{-1} and used for crystallization.

Selenomethionine-derivative NSR protein was expressed using *E. coli* strain BL21 (DE3) cultured in M9 minimal medium supplemented with 100 mg l^{-1} lysine, 100 mg l^{-1} phenylalanine, 100 mg l^{-1} threonine, 50 mg l^{-1} isoleucine, 50 mg l^{-1} leucine, 50 mg l^{-1} valine and 25 mg l^{-1} selenomethionine (Acros). Expression and purification procedures were performed as for wild-type NSR. Full incorporation of selenomethionine was verified by ESI mass spectrometry.

2.2. Protein crystallization

To obtain the NSR–SAM complex, NSR protein was incubated with SAM (New England Biolabs) on ice for 1 h with a 1:10 molar ratio of protein:SAM. Initial crystallization trials were performed using Crystal Screen, Index, SaltRX and PEG/Ion kits from Hampton Research and Wizard I and II kits from Emerald BioSystems at 293 K. These initial screens were set up using the hanging-drop vapour-diffusion method by mixing 1 µl protein solution and 1 µl reservoir solution. Initial conditions yielding crystals were further optimized by variation of the protein concentration, pH, precipitants and additives. We set up a total of approximately 600 conditions for optimization and screened three concentrations: 10, 6 and 4 mg ml^{-1}.

2.3. Data collection and processing

All crystals were mounted in nylon loops and flash-frozen in liquid nitrogen using reservoir buffer as cryoprotectant. Data collection was carried out on beamlines BL17A at Photon Factory, Japan and BL17U at SSRF, People's Republic of China using crystals that had been flash-frozen at 100 K in a stream of cold nitrogen gas. A CCD detector was used. Data were indexed, integrated and scaled using the program *HKL*-2000 (Otwinowski & Minor, 1997). The refinement σ cutoff was set to 5 during data processing.

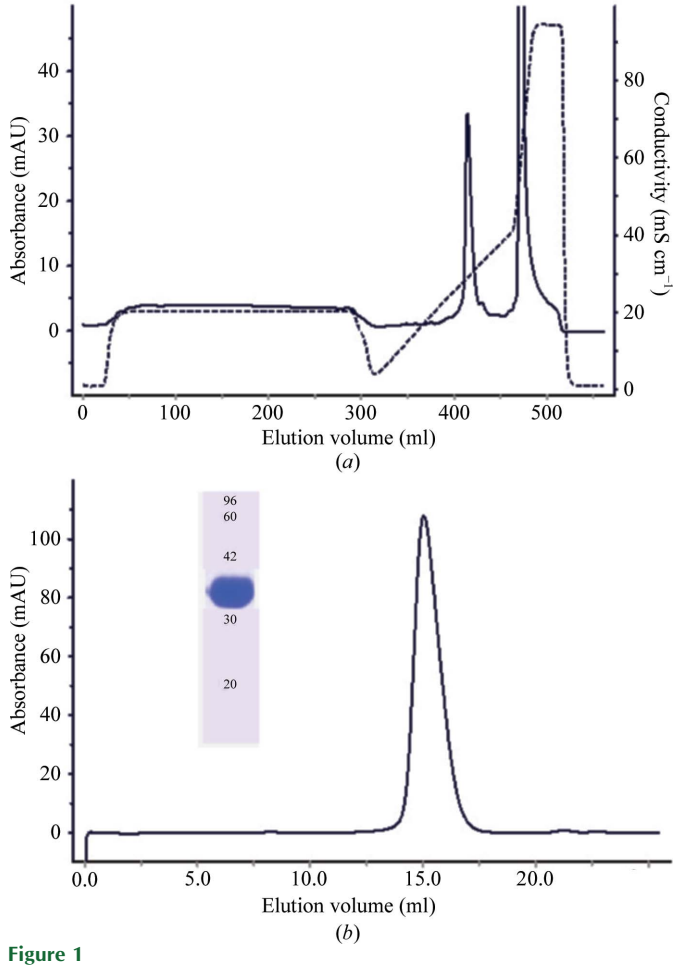

Figure 1
NSR protein purification. (*a*) Ion-exchange (Source 15Q, GE Healthcare) profile of NSR protein. (*b*) Gel-filtration (Superdex 200, 10/300 GL, GE Healthcare) profile of NSR protein. Inset: one of the peak fractions was analyzed by SDS–PAGE with Coomassie Blue staining. Molecular weights are indicated in kDa.

3. Results and discussion

Recombinant NSR protein was expressed, purified to homogeneity and used for crystallization (Figs. 1*a* and 1*b*). The purified NSR protein was estimated to be >98% pure (Fig. 1*c*). The NSR protein precipitated above a concentration of 2 mg ml^{-1} in gel-filtration buffer containing 25 m*M* Tris pH 8.0, 150 m*M* NaCl. We successfully improved the solubility of NSR in solution by increasing the NaCl concentration to 250 m*M*, which allowed NSR to be concentrated to >10 mg ml^{-1} and used for crystallization trials. The crystals (Fig. 2) used for data collection were obtained by mixing 1 µl protein solution (4 mg ml^{-1}) with 1 µl reservoir solution containing 0.35 *M* ammonium chloride, 24%(*w*/*v*) PEG 3350, 0.1 *M* MES pH 5.7 at 293 K. Large single cubic crystals appeared after 2 d and reached their maximum dimensions 6 d later. Crystals of NSR protein complexed with SAM and of the selenomethionine derivative of NSR were grown under similar conditions.

In order to overcome any potential difficulties in using molecular replacement for structure determination, we produced crystals of selenomethionine-derivative NSR protein. Se-SAD (single-wavelength anomalous diffraction; Hendrickson, 1991) data were collected at a wavelength of 0.9788 Å using a single crystal. Data sets for the apo form of NSR, for NSR complexed with SAM and for SeMet-labelled NSR were also collected; the diffraction extended to 1.90, 1.95 and 2.25 Å resolution, respectively (Fig. 3). The crystals of SeMet-labelled NSR belonged to space group $P2_1$, with unit-cell parameters a = 64.6, b = 69.6, c = 64.9 Å, β = 117.8°. Two monomers are expected in the asymmetric unit, with a solvent content of about 41%. Data-collection statistics are summarized in Table 1. The structures were determined by the SAD phasing method and will be published elsewhere; molecular replacement was unsuccessful.

Table 1
Diffraction data statistics.

Values in parentheses are for the highest resolution shell.

	NSR	NSR–SAM	SeMet NSR
Wavelength (Å)	1.0055	0.9794	0.9788
Resolution (Å)	50.00–1.90 (1.97–1.90)	50.00–1.95 (2.02–1.95)	50.00–2.25 (2.33–2.25)
Space group	$P2_1$	$P2_1$	$P2_1$
Unit-cell parameters (Å, °)	a = 64.9, b = 69.2, c = 64.8, β = 117.8	a = 63.7, b = 69.2, c = 64.4, β = 117.6	a = 64.6, b = 69.6, c = 64.9, β = 117.8
Completeness (%)	97.4 (83.8)	99.2 (97.8)	99.5 (100.0)
$R_{\rm merge}$† (%)	5.8 (32.5)	5.3 (43.2)	9.1 (52.1)
$I/\sigma(I)$	33.3 (4.3)	31.7 (3.4)	20.4 (4.8)
Redundancy	7.1 (5.0)	7.2 (5.7)	7.6 (7.6)
Total No. of reflections	276005 (16845)	260071 (20229)	181982 (18134)
No. of unique reflections	38874 (3369)	36121 (3549)	23945 (2386)

† $R_{\rm merge} = \sum_{hkl}\sum_i |I_i(hkl) - \langle I(hkl)\rangle| / \sum_{hkl}\sum_i I_i(hkl)$, where $I_i(hkl)$ is the ith measurement of the intensity of reflection hkl and $\langle I(hkl)\rangle$ is the mean intensity of reflection hkl (Hall & McMahon, 2006).

The crystal structures of NSR and of NSR in complex with SAM may reveal the substrate-recognition and molecular mechanism of RNA methylation mediated by nosiheptide-resistance methyltransferase. It will also expand our understanding of the mechanisms of antibiotic resistance.

We thank the staff members of beamlines BL17U at SSRF (China) and BL17A at Photon Factory (Japan) for their help with data collection. This work was supported by grants from the Shanghai Municipal Natural Science Foundation (10ZR1402800), the National

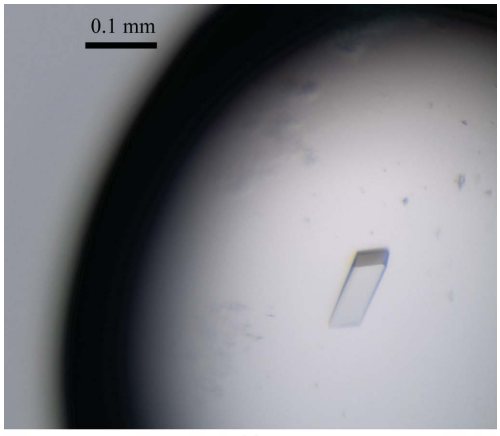

(*a*)

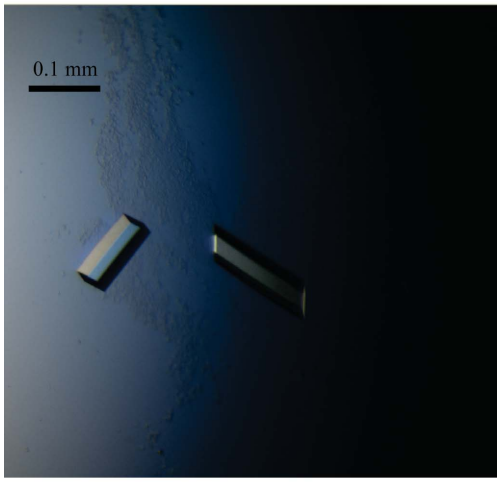

(*b*)

Figure 2
Crystals of selenomethionine-derivative NSR (*a*) and of NSR in complex with SAM (*b*) grown in 0.35 *M* ammonium chloride, 24%(*w*/*v*) PEG 3350, 0.1 *M* MES pH 5.7 at 293 K. The scale bar represents 0.1 mm.

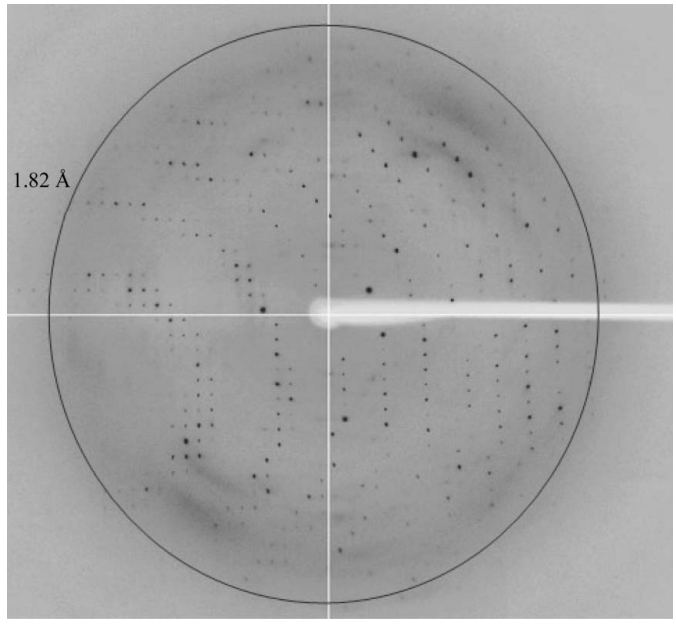

Figure 3
X-ray diffraction pattern of the crystal of selenomethionine-derivative NSR. The ring indicates a resolution of 1.82 Å.

Natural Science Foundation of China (30870493), the National Basic Research Program of China (2009CB918600), the Shanghai Pujiang Program (08PJ14010), the Ministry of Science and Technology of China (2009ZX09503-006) and the Shanghai Leading Academic Discipline Project (B111).

References

Bechthold, A. & Floss, H. G. (1994). *Eur. J. Biochem.* **224**, 431–437.
Cromwell, G. L., Stahly, T. S., Speer, V. C. & O'Kelly, R. (1984). *J. Anim. Sci.* **59**, 1125–1128.
Dunstan, M. S., Hang, P. C., Zelinskaya, N. V., Honek, J. F. & Conn, G. L. (2009). *J. Biol. Chem.* **284**, 17013–17020.
Endo, T. & Yonehara, H. (1978). *J. Antibiot.* **31**, 623–625.
Farrow, K. A., Lyras, D. & Rood, J. I. (2000). *Antimicrob. Agents Chemother.* **44**, 411–413.
Finn, R. D., Tate, J., Mistry, J., Coggill, P. C., Sammut, S. J., Hotz, H. R., Ceric, G., Forslund, K., Eddy, S. R., Sonnhammer, E. L. & Bateman, A. (2008). *Nucleic Acids Res.* **36**, D281–D288.
Gutell, R. R., Larsen, N. & Woese, C. R. (1994). *Microbiol. Rev.* **58**, 10–26.
Hall, S. R. & McMahon, B. (2006). Editors. *International Tables for Crystallography*, Vol. *G*, 1st online edition. Chester: International Union of Crystallography.
Harms, J. M., Wilson, D. N., Schluenzen, F., Connell, S. R., Stachelhaus, T., Zaborowska, Z., Spahn, C. M. & Fucini, P. (2008). *Mol. Cell*, **30**, 26–38.
Hendrickson, W. A. (1991). *Science*, **254**, 51–58.
Lentzen, G., Klinck, R., Matassova, N., Aboul-ela, F. & Murchie, A. I. (2003). *Chem. Biol.* **10**, 769–778.
Li, Y., Dosch, D. C., Strohl, W. R. & Floss, H. G. (1990). *Gene*, **91**, 9–17.
Michel, G., Sauve, V., Larocque, R., Li, Y., Matte, A. & Cygler, M. (2002). *Structure*, **10**, 1303–1315.
Mosbacher, T. G., Bechthold, A. & Schulz, G. E. (2005). *J. Mol. Biol.* **345**, 535–545.
Ohta, T. & Hasegawa, M. (1993). *Gene*, **127**, 63–69.
Otwinowski, Z. & Minor, W. (1997). *Methods Enzymol.* **276**, 307–326.
Prangé, T., Ducruix, A., Pascard, C. & Lunel, J. (1977). *Nature (London)*, **265**, 189–190.
Robinow, C. & Kellenberger, E. (1994). *Microbiol. Rev.* **58**, 211–232.
Roje, S. (2006). *Phytochemistry*, **67**, 1686–1698.
Thompson, J. & Cundliffe, E. (1980). *J. Bacteriol.* **142**, 455–461.
Wimberly, B. T., Guymon, R., McCutcheon, J. P., White, S. W. & Ramakrishnan, V. (1999). *Cell*, **97**, 491–502.